Selective n-Type Doping of Graphene by Photo-patterned Gold Nanoparticles

Sung Huh,[†] Jaesung Park,[†] Kwang S. Kim,[†,*] Byung Hee Hong,[‡,§,*] and Seung Bin Kim[†,*]

[†]Department of Chemistry, Pohang University of Science and Technology, Pohang 790-784, Korea, [‡]SKKU Advanced Institute of Nanotechnology (SAINT) and Center for Human Interface Nano Technology (HINT), and [§]Department of Chemistry, Sungkyunkwan University, Suwon 440-746, Korea

ABSTRACT Selective n-type doping of graphene is developed by utilizing patternable gold nanoparticles functionalized with photoreactive cinnamate moieties. The gold nanoparticles can be regularly patterned on the graphene by UV-induced cross-linking of cinnamate, which provides a convenient method to control the optical and electrical properties of graphene site-specifically. The strong n-type doping of graphene covered with the patterned gold nanoparticles was confirmed by Raman, X-ray photoelectron spectroscopy, and electron transport measurements. We believe that our method would find numerous applications in the area of graphene-based optoelectronics including light-emitting devices, solar cells, and optical sensors.

KEYWORDS: graphene · gold nanoparticles · doping · Raman enhancement · electron transport measurement

Despite the recent intensive research on the unique electrical, mechanical, and chemical properties of graphene,[1−4] n-doping modulation has been less investigated compared to p-doping, although both p/n-doping methods are of importance to optimize the characteristics and performance of graphene-based electronic devices.[5−12] In particular, the spatially selective doping of graphene is essential to fabricate integrated devices with complicated architecture such as logic gates or p−n diodes.[13−20] The previous patterned doping methods mostly used positive resists that can be patterned by e-beam or photolithography. In this case, more than five steps including spin coating, UV-exposure, developing, doping, and lift-off are needed,[21−24] which is not efficient compared to direct patterning methods.[25−28] Thus we report a simple method to control the n-doping characteristics of graphene site-specifically utilizing gold nanoparticles not only as negative resists but as n-dopants. Recently, the large-scale synthesis of graphene films has been intensively studied,[29,30] enabling the use of graphene for macroscopic devices such as touch screen panels.[31,32] In addition, the batch fabrication and the site-specific doping of microscale graphene devices are important as well for practical applications. In this regard, our direct patterned doping method would be suitable for the large-scale fabrication and functionalization of graphene-based integrated circuits.

RESULTS AND DISCUSSION

We developed photo-patternable gold nanoparticles decorated with cinnamates as photoreactive groups (to be briefly denoted as Ci-AuNPs) that can be covalently cross-linked during the UV irradiation process.[33,34] Figure 1a shows the patterning procedure of the Ci-AuNPs on the graphene surface. At first, the graphene film synthesized by chemical vapor deposition (CVD) methods was prepared on a SiO_2/Si substrate. The single-layer graphenes were confirmed by Raman spectroscopy with 514 nm excitation, as shown in Figure 1b. The G band at 1582 cm^{-1} and 2D band at 2679 cm^{-1}, but no D band, were observed in the Raman spectrum. The intensity ratio of 2D to G band (I(2D)/I(G)) of 3.58 supported the identification of the single-layer graphenes used in this work.[35,36] After spin coating of Ci-AuNPs in toluene on the graphene surface, the nanoparticles are cross-linked selectively by UV irradiation through a shadow mask. Finally, the patterned Ci-AuNPs remained on the graphene surface after a careful lift-off step.

The Ci-AuNPs exist separately and confirmed that their average size was 3.2 ± 0.2 nm, as calculated by scanning electron microscopy (SEM) image (Figure 2a). The resulting particles showed good solubility in many organic solvents, including chloroform, benzene, and toluene. Figure 2b shows Fourier transform infrared (FTIR) spectra of DHDCI, cinnamate-containing disulfide (*i.e.*, 3,4-dithiahexane-1,6-dicinnamate, DHDCI), which covered the gold nanoparticles, and Ci-AuNPs.[37] As can be seen, bands at 1710 cm^{-1} due to the vinylene C=C stretching vibration and 1637 cm^{-1} due to the C=O stretching vibration in the spectrum

* Address correspondence to sbkim@postech.edu (S.B.K.), byunghee@skku.edu (B.H.H.), kim@postech.edu (K.S.K.).

Received for review December 18, 2010 and accepted April 5, 2011.

Published online April 05, 2011
10.1021/nn1035203

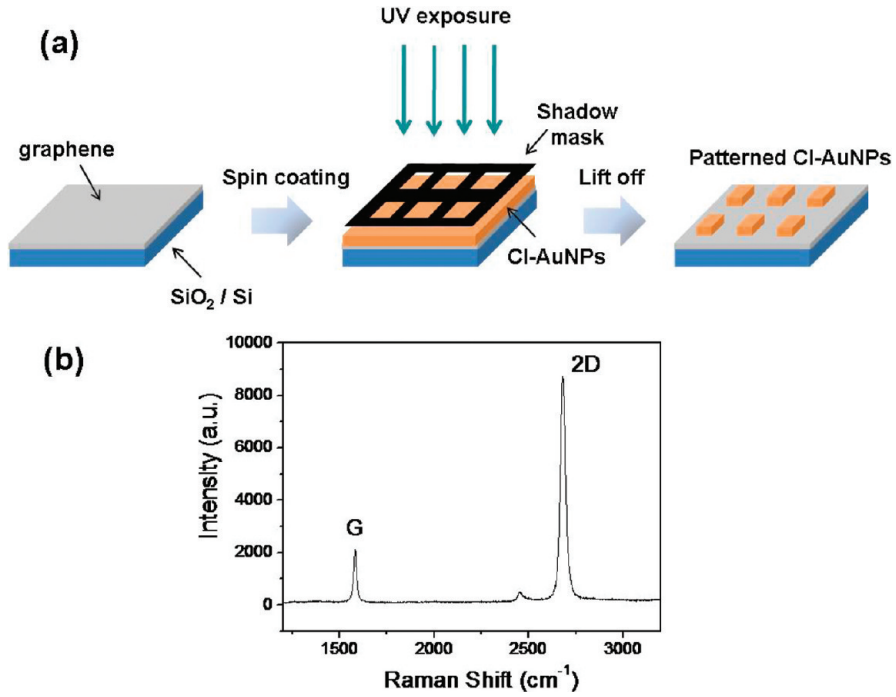

Figure 1. (a) Patterning procedure of Ci-AuNPs on graphene. (b) Raman spectrum of single-layer graphene.

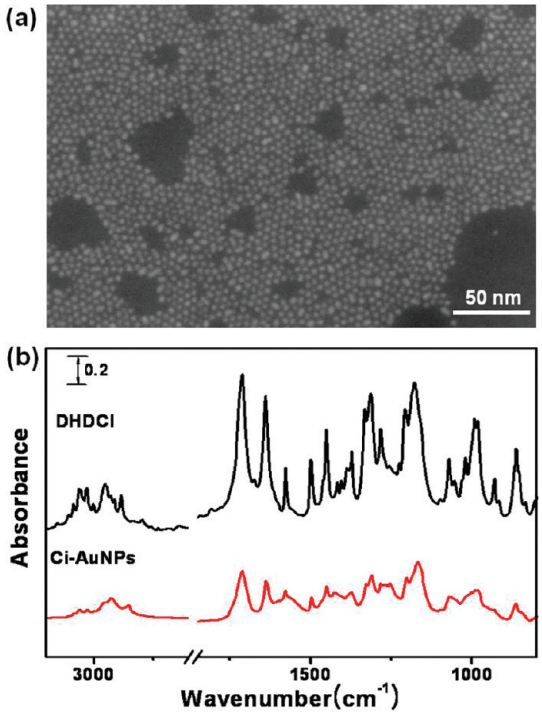

Figure 2. Characterization of Ci-AuNPs: (a) SEM image and (b) FTIR spectra of DHDCI and Ci-AuNPs.

of Ci-AuNPs resemble those of DHDCI, providing clear evidence that DHDCI existed on the particles. The Raman spectrum provides spectroscopic evidence of the binding on the gold surface, showing the absence of the S−S stretching mode of DHDCI in the spectrum of Ci-AuNPs (data not shown).[38] Consequently, the results show the coverage of DHDCI on the AuNPs surfaces.

The patterned images of the Ci-AuNPs on graphene after UV irradiation were obtained by optical microscopy (OM), SEM (Figure 3), and atomic force microscopy (AFM) (Figure 4). The exposed area of the film remains, whereas the masked area is removed after the lift-off process, resulting in photolithography patterning of Ci-AuNPs on graphene. The pattern widths of the masks are 7.5 and 19 μm for Figure 3a and b, respectively. After performing experiments for various UV exposure times, we found that the patterned features were the clearest for irradiation of $\sim$3 J/cm^2. We have confirmed the existence of the gold nanoparticles on the patterned area using energy dispersive X-ray (EDX) spectroscopy. The thickness of the Ci-AuNPs patterns can be controlled by the concentration and the spin-coating rate of the Ci-AuNP-dispersed toluene solution. Figure 4 shows the AFM images and the height profiles of Ci-AuNPs film patterns with respect to the concentrations of Ci-AuNPs solutions, showing that the higher concentration yields thicker patterns. We observed that a concentration higher than 2 wt % results in the bold edge features as shown in Figure 4b, which is due to the inhomogeneous depth profile of UV intensity, affecting the cross-linked amount of Ci-AuNPs. As a result, the cross-linked outer shell of the pattern collapses as the unreacted core region is removed by solvent.

A clear enhancement in the Raman intensity on the patterned area was observed, which is due to the strong surface-enhanced Raman scattering (SERS) at graphene−gold interfaces.[39−42] The boxed area in Figure 5a was mapped by confocal Raman spectroscopy with 633 nm excitation. Two characteristic peaks

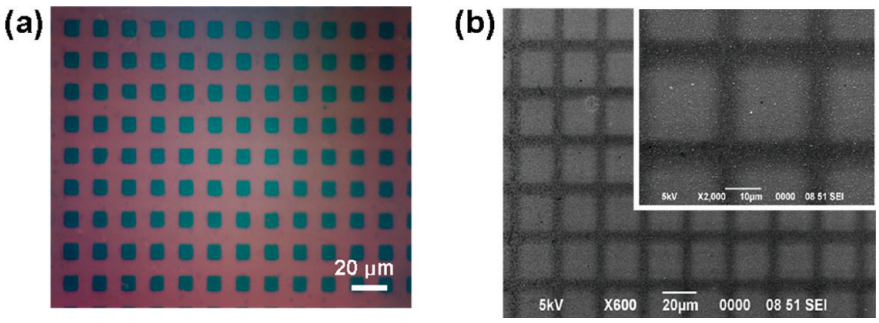

Figure 3. (a) OM image and (b) SEM image of patterned Ci-AuNPs on graphene.

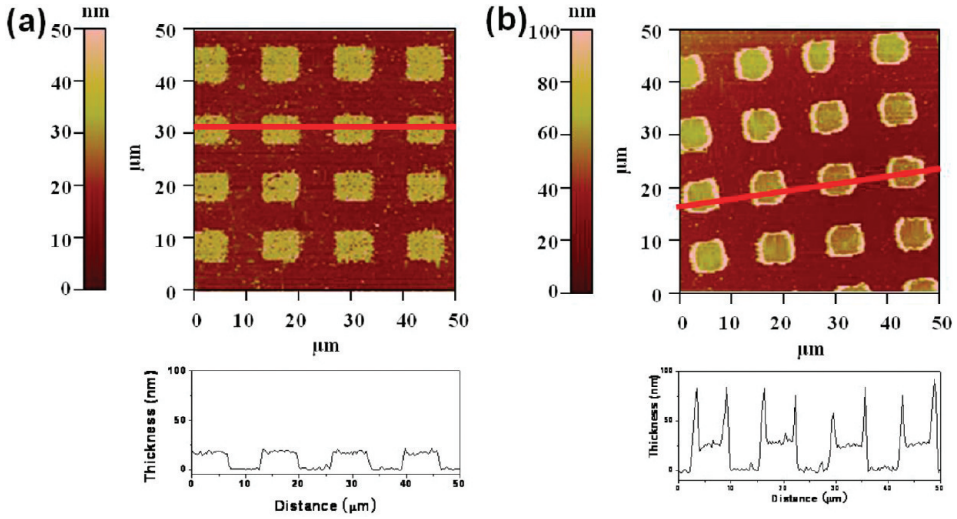

Figure 4. AFM images and height profiles of the Ci-AuNPs patterns for 2 wt % (a) and 3 wt % (b) Ci-AuNPs solution.

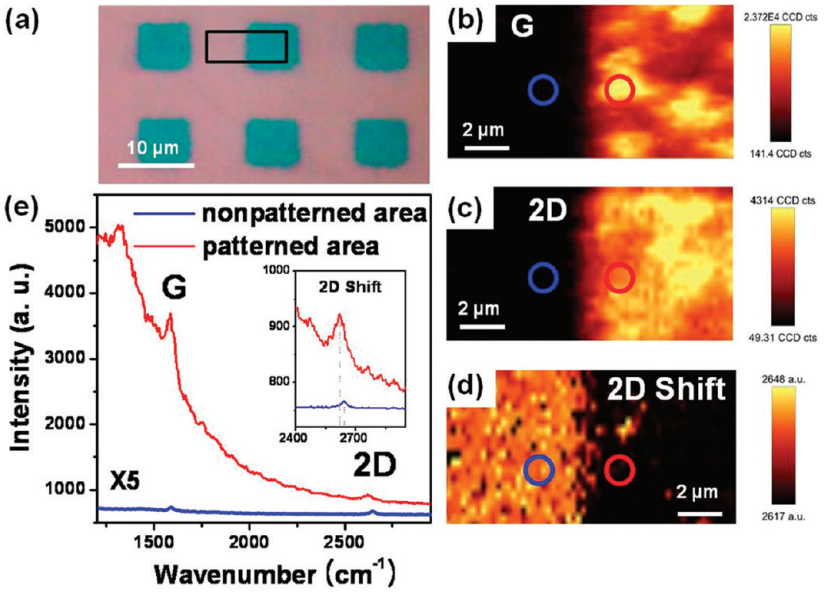

Figure 5. (a) OM image of Ci-AuNPs on graphene. Black box is the selected area for Raman mapping. Raman images was mapped with the integrated intensities of (b) G bands, (c) 2D bands, and (d) shifts of the center position of 2D bands. (e) Raman spectra of patterned (red circle) and nonpatterned (blue circle) areas. The inset shows the downshift of the 2D band on the patterned area.

of graphene, the G band and 2D band,[43] were monitored to confirm the Raman enhancement in the patterned area (Figure 5b,c), showing that the Au patterning increases the G and 2D band intensities

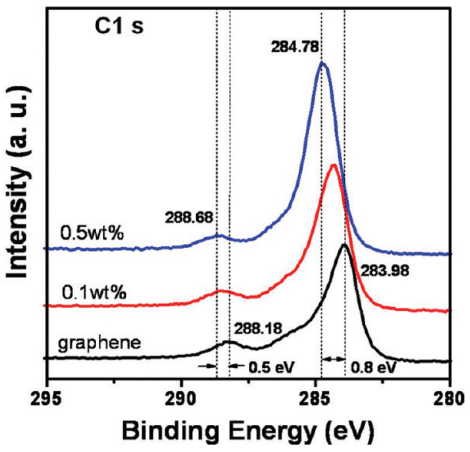

Figure 6. XPS spectra of the graphene and the Ci-AuNPs-coated graphene with different concentrations, showing the higher binding energy shift of C1s electrons induced by strong n-doping.

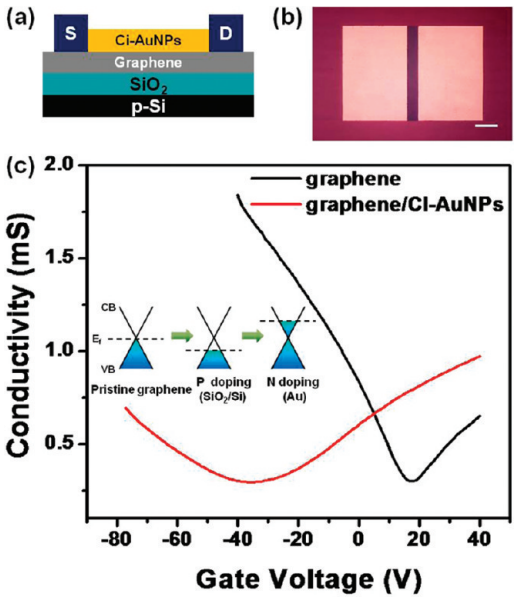

Figure 7. (a) Schematic diagram of the device with graphene and Ci-AuNPs. (b) OM image of the graphene field effect transistor with a Ci-AuNPs coating. Scale bar, 100 μm. (c) Conductivity–gate voltage curve of the graphene and the Ci-AuNPs-coated graphene measured at V_{sd} = 10 mV. The inset shows the relationship between the Fermi energy shift and p/n-doping levels of graphene.

by 70.3 and 6.7 times, respectively (Figure 5e). In particular, the 2D bands on the pattered area shifted down from 2640 to 2620 cm^{-1}, indicating that the gold nanoparticles selectively induced n-type doping of graphene in the patterned area.[35,36] This also can be confirmed by the XPS spectra in Figure 6, where the main C1s peak related to pure sp^2 carbon–carbon bonds shifted from 284.78 to 283.98 eV as the graphene is n-doped by gold nanorpaticles.[11,44] The sp^3-related peak upshifted by ~0.5 eV also confirms the n-doping effect as the electron-rich gold nanoparticles allowed the electron transfer to graphene. The higher concentration of AuNPs on the graphene leads to a higher binding energy, *i.e.*, the stronger n-doping effect as shown in Figure 6. Therefore, the results represent the tunable doping method of graphene by the AuNPs, with the possibility to control the optical properties of graphene including the Raman enhancement.

The doping effect of gold nanoparticles on graphene was investigated by transport measurements in high vacuum (~10^{-6} Torr), where Dirac voltages (the gate dependence of minimum conductivity) shift depending on electron or hole doping levels.[42,43] The device structure with Ci-AuNPs-coated graphene as a semiconductor layer is represented in Figure 7a,b (a detailed explanation for device fabrication is mentioned in the Methods section). Figure 7c shows the clear negative shift of the Dirac voltages before and after the Ci-AuNPs pattering on graphene (spin-coated with 0.5 wt % Ci-AuNPs solution), which agrees with the previous report on the effect of Au deposition on the transport properties of graphene.[45–47] To support the n-doping effect of the Ci-AuNPs on the graphene, we tried to examine the electrical performances of graphene with respect to the concentration of Ci-AuNPs solutions. The resulting data showed a tendency toward negative shift of the Dirac voltages as

TABLE 1. Dirac Voltage and Mobility Changes Due to the Treatment of Ci-AuNPs on the Graphene Surface

	graphene	graphene/Ci-AuNPs
Dirac voltage (V)	17.5	−35.6
hole mobility (10^3 cm^2/(V s))	3.27	1.54
electron mobility (10^3 cm^2/(V s))	1.71	1.13

the concentration of Ci-AuNPs solution treated on the graphene was increased. A more detailed study is desired to understand the doping mechanism of the graphene with the AuNPs in the next project. The field-effect transistor (FET) mobility of holes decreases more than that of electrons (Table 1). We suggest that the conductance asymmetry arises from the imbalanced carrier injection from the device's electrodes caused by misalignment of the electrode and channel neutrality points, as mentioned in the previous research.[48] It is assumed that there is an unknown, complicated doping system in this experiment, which is expected to be defined more clearly. As a result, we conclude that the AuNPs act as electron donors, leading to the strong n-doping of graphene.

In conclusion, we devised a new method to n-dope graphene site-specifically using photo-patternable gold nanoparticles functionalized with cinnamate moieties that can be cross-linked by UV irradiation. The Raman, XPS, and electron transport measurements support that the electrons are considerably transferred from Au to graphene, resulting in the strong n-type doping of graphene. This simple doping method

provides a convenient method to control the optical and electrical properties of graphene site-specifically, which would find various electronic device applications based on graphene in the future.

METHODS

Materials. Cinnamoyl chloride (98%), bis(11-hydroxyundecyl) disulfide (99%), triethylamine (99%), tetraoctylammonium bromide (99%), gold(III) chloride hydrate (99.999%), and sodium borohydride (98%) were purchased from Aldrich. All reagents were used without any further purification.

Synthesis of Graphene. The graphene films were synthesized on Cu foils by CVD.[29−32] The Cu foils (25 μm thickness) were placed in a quartz tube under an argon atmosphere. The temperature was raised to 1000 °C, and the reaction gas mixture of CH_4 and H_2 was flowed. Then the foils were cooled to room temperature at a rate of ~10 °C. Since the graphene layers are formed on both sides of a Cu foil, the back-side graphene should be removed by O_2 plasma etching after protecting the front graphene layer with PMMA. After etching the Cu foil in an ammonium persulfate solution for ~10 h, the graphene layer was transferred onto a target substrate. Finally, the PMMA layer was removed by acetone.

Preparation of Ci-AuNPs. Gold nanoparticles covered with cinnamate-containing disulfide (DHDCI) synthesized in our recent work[37] were prepared by using the two-phase Brust−Schiffrin method.[49,50] An aqueous solution of $HAuCl_4$ (0.039 g, 30 mM) and a solution of tetraoctylammonium bromide (0.219 g, 50 mM) in toluene (8 mL) as a phase-transfer reagent were mixed and stirred until the aqueous phase was colorless. The DHDCI (0.041 g, 30 mM) solution with toluene was added to the above solution with stirring. Upon vigorous stirring, an aqueous solution of $NaBH_4$ was added dropwise to the mixture and then allowed to react for three hours. The gold nanoparticles were finally extracted from the organic phase, confirmed by scanning electron microscopy. The immobilization of DHDCI on the surface of the nanoparticles was confirmed by Fourier transform infrared spectroscopy

Measurements. The FTIR spectroscopic measurements were carried out at a spectral resolution of 4 cm^{-1} by using an FTIR spectrometer (Bomem DA8) equipped with a liquid-nitrogen-cooled mercury−cadmium−telluride detector. The FTIR samples were coated onto NaCl windows [25 mm (diameter) × 2 mm (thickness)]. Optical microscopy images were collected by using a microscope (Olympus Co.). The patterned Ci-AuNPs film was also characterized by using a SEM (JSM-7401F; JEOL) operating at an accelerating voltage of 5 kV. The energy-dispersive X-ray spectroscopy mode of SEM was used for elemental analyses of the patterned films. The morphologies of the films were determined by using atomic force microscopy with a noncontact mode (Veeco Digital Instruments Dimension 3100). The Raman spectra were acquired using an Alpha 300s (WITEC, Germany) with an Ar laser of 514 nm and a HeNe laser of 633 nm at a power of 5 mW and pixel size of 250 nm.

Raman images were mapped by the integrated intensities of G and 2D bands from 1530 to 1650 cm^{-1} and from 2570 to 2690 cm^{-1}, respectively. X-ray photoelecton spectroscopy (XPS) was used for measurement of the binding energy of the carbon bond (K-Alpha, Thermo Electron). The gate-dependent conductivity of the films was measured with a probe station at room temperature. A high-vacuum (10^{-6} Torr) system was used for more reproducible measurements than ambient conditions.[51]

Device Fabrication for Transport Measurement. Electrical measurements were performed on the newly fabricated devices by using heavily doped p-type Si wafers as the gate electrodes and silicon dioxide (SiO_2) of 150 nm thickness (capacitance = 20 nF cm^{-2}) as the gate dielectric layer. The 30 nm thick gold source and drain electrodes were structured in top-contact transistors with a channel length of 50 μm and a width of 800 μm. A 5 nm thick titanium layer was used for adhesion of the gold electrodes. The graphene layer was transferred onto the substrate and located between the source and drain electrodes as a channel layer. To dope the graphene, a simple spin-casting method for the Ci-AuNPs solution was used to cover the graphene surface with a thicknesses in the range of a few nanometers.

Patterning Process of Ci-AuNPs on a Graphene Sheet. To pattern Ci-AuNPs on a graphene layer, a 2 wt % toluene solution of the nanoparticles was spin-coated onto a graphene-transferred Si/SiO_2 wafer (1 cm × 1 cm) for 1 min at 2500 rpm. After the film had been held under vacuum for 24 h, a microsized square-patterned shadow mask was attached onto the film surface before irradiation with UV light. A high-pressure 1.0 kW Hg lamp system (Altech, model ALHg-1000) was employed as the UV-light source, together with an optical filter (Milles Griot, model 03-FCG-179), which transmits a band beam of 260−380 nm. The optically filtered UV-light intensity was 10 mW/cm^2. The exposure dose was measured by using a photometer (model IL 1350). After removing the shadow mask from the film surface, the film was briefly washed with toluene and dried. The patterns were examined with optical microscopy, SEM, and AFM.

Acknowledgment. This study was supported by the Second Stage of the Brain Korea 21 Project and National Research Foundation of Korea (NRF) through the Ministry of Education, Science and Technology (National Honor Scientist Program: 2010-0020414, Converging Research Center Program: 2010K001066, Basic Science Research Program: 2009-0089030).

REFERENCES AND NOTES

1. Novoselov, K. S.; Geim, A. K.; Morozov, S. V.; Jiang, D.; Zhang, Y.; Dubonos, S. V.; Grigorieva, I. V.; Firsov, A. A. Electric Field Effect in Atomically Thin Carbon Films. *Science* **2004,** *306*, 666–669.
2. Geim, A. K.; Novoselov, K. S. The Rise of Graphene. *Nat. Mater.* **2007,** *6*, 183–191.
3. Novoselov, K. S.; Geim, A. K.; Morozov, S. V.; Jiang, D.; Katsnelson, M. I.; Grigorieva, I. V.; Dubonos, S. V.; Firsov, A. A. Two-dimensional Gas of Massless Dirac Fermions in Graphene. *Nature* **2005,** *438*, 197–200.
4. Zhang, Y.; Tan, Y. W.; Stormer, H. L.; Kim, P. Experimental Observation of the Quantum Hall Effect and Berry's Phase in Graphene. *Nature* **2005,** *438*, 201–204.
5. Martins, T. B.; Miwa, R. H.; Silva, A. J. R.; Fazzio, A. Electronic and Transport Properties of Boron-Doped Graphene Nanoribbons. *Phys. Rev. Lett.* **2007,** *98*, 196803.
6. Wehling, T. O.; Novoselov, K. S.; Morozov, S. V.; Vdovin, E. E.; Katsnelson, M. I.; Geim, A. K.; Lichtenstein, A. I. Molecular Doping of Graphene. *Nano Lett.* **2008,** *8*, 173–177.
7. Wang, X.; Li, X.; Zhang, L.; Yoon, Y.; Weber, P. K.; Wang, H. Guo, J.; Dai, H. N-Doping of Graphene Through Electrothermal Reactions with Ammonia. *Science* **2009,** *324*, 768–771.
8. Schedin, F.; Geim, A. K.; Morozov, S. V.; Hill, E. W.; Blake, P.; Katsnelson, M. I.; Novoselov, K. S. Detection of Individual Gas Molecules Adsorbed on Graphene. *Nat. Mater.* **2007,** *6*, 652–655.
9. Guo, B.; Liu, Q.; Chen, E.; Zhu, H.; Fang, L.; Gong, J. R. Controllable N-Doping of Graphene. *Nano Lett.* **2010,** *10*, 4975–4980.
10. Wei, D.; Liu, Y.; Wang, Y.; Zhang, H.; Huang, L.; Yu, G. Synthesis of N-Doped Graphene by Chemical Vapor Deposition and Its Electrical Properties. *Nano Lett.* **2009,** *9*, 1752–1758.
11. Lin, Y. C.; Lin, C. Y.; Chiu, P. W. Controllable Graphene N-doping with Ammonia Plasma. *Appl. Phys. Lett.* **2010,** *96*, 133110.
12. Li, N.; Wang, Z.; Zhao, K.; Shi, Z.; Gu, Z.; Xu, S. Large Scale Synthesis of N-Doped Multi-Layered Graphene Sheets

by Simple Arc-Discharge Method. *Carbon* **2010,** *48*, 255–259.
13. Huard, B.; Sulpizio, J. A.; Stander, N.; Todd, K.; Yang, B.; Goldhaber-Gordon, D. *Phys. Rev. Lett.* **2007,** *98*, 236803.
14. Williams, J. R.; DiCarlo, L.; Marcus, C. M. Quantum Hall Effect in a Gate-Controlled *p-n* Junction of Graphene. *Science* **2007,** *317*, 638–641.
15. Oezyilmaz, B.; Jarillo-Herrero, P.; Efetov, D.; Abanin, D.; Levitov, L. S.; Kim, P. Electronic Transport and Quantum Hall Effect in Bipolar Graphene *p-n-p* Junctions. *Phys. Rev. Lett.* **2007,** *99*, 166804.
16. Bangert, U.; Bleloch, A.; Gass, M. H.; Seepujak, A.; van den Berg, J. Doping of Few-layered Graphene and Carbon Nanotubes using Ion Implantation. *Phys. Rev. B* **2010,** *81*, 245423.
17. Koehler, F. M.; Jacobsen, A.; Ensslin, K.; Stampfer, C.; Stark, W. J. Selective Chemical Modification of Graphene Surfaces: Distinction between Single- and Bilayer Graphene. *Small* **2010,** *6*, 1125–1130.
18. Wei, D.; Liu, Y. Controllable Synthesis of Graphene and Its Applications. *Adv. Mater.* **2010,** *22*, 3225–3241.
19. Lohmann, T.; Klitzing, K. V.; Smet, J. H. Four-Terminal Magneto-Transport in Graphene p-n Junctions Created by Spatially Selective Doping. *Nano Lett.* **2009,** *9*, 1973–1979.
20. Ohta, T.; Bostwick, A.; Seyller, T.; Horn, K.; Rotenberg, E. Controlling the Electronic Structure of Bilayer Graphene. *Science* **2006,** *313*, 951–954.
21. Gates, B. D.; Xu, Q.; Stewart, M.; Ryan, D.; Willson, C. G.; Whitesides, G. M. New Approaches to Nanofabrication: Molding, Printing, and Other Techniques. *Chem. Rev.* **2005,** *105*, 1171–1196.
22. Muller, C. D.; Falcou, A.; Reckefuss, N.; Rojahn, M.; Wiederhirn, V.; Rudati, P.; Frohne, H.; Nuyken, O.; Becker, H.; Meerholz, K. Multi-Colour Organic Light-Emitting Displays by Solution Processing. *Nature* **2003,** *421*, 829–833.
23. Huang, S.; Dai, L.; Mau, A. W. H. Controlled Fabrication of Large-Scale Aligned Carbon Nanofiber/Nanotube Patterns by Photolithography. *Adv. Mater.* **2002,** *14*, 1140–1143.
24. Yang, Y.; Huang, S.; He, H.; Mau, A. W. H.; Dai, L. Controlled Fabrication of Large-Scale Aligned Carbon Nanofiber/Nanotube Patterns by Photolithography. *J. Am. Chem. Soc.* **1999,** *121*, 10832–10833.
25. Wu, C. C.; Marcy, D.; Lu, M. H.; Sturm, J. C. *Appl. Phys. Lett.* **1998,** *72*, 519–521.
26. Piner, R. D.; Zhu, J.; Xu, F.; Hong, S. H.; Mirkin, C. A. "Dip-Pen" Nanolithography. *Science* **1999,** *283*, 661–663.
27. Behl, M.; Seekamp, J.; Wankovych, S.; Torres, C. M. S.; Zentel, R.; Ahopelto, J. Towards Plastic Electronics: Patterning Semiconducting Polymers by Nanoimprint Lithography. *Adv. Mater.* **2002,** *14*, 588–591.
28. Hua, F.; Sun, Y.; Gaur, A.; Meitl, M. A.; Bilhaut, L.; Rotkina, L.; Wang, J.; Geil, P.; Shim, M.; Rogers, J. A.; *et al.* Polymer Imprint Lithography with Molecular-Scale Resolution. *Nano Lett.* **2004,** *4*, 2467–2471.
29. Kim, K. S.; Zhao, Y.; Jang, H.; Lee, S. Y.; Kim, J. M.; Kim, K. S.; Ahn, J. H.; Kim, P.; Choi., J. Y.; Hong, B. H. Large-scale Pattern Growth of Graphene Films for Stretchable Transparent Electrodes. *Nature* **2009,** *457*, 706–710.
30. Li, X.; Zhu, Y.; Cai, W.; Borysiak, M.; Han, B.; Chen, D.; Piner, R. D.; Colombo, L.; Ruoff, R. S. Transfer of Large-Area Graphene Films for High-Performance Transparent Conductive Electrodes. *Nano Lett.* **2009,** *9*, 4359–4363.
31. Reina, A.; Jia, X.; Ho, J.; Nezich, D.; Son, H.; Bulovic, V.; Dresselhaus, M. S.; Kong, J. Large Area, Few-Layer Graphene Films on Arbitrary Substrates by Chemical Vapor Deposition. *Nano Lett.* **2009,** *9*, 30–35.
32. Bae, S.; Kim, H.; Lee, Y.; Xu, X.; Park, J. S.; Zheng, Y.; Balakrishnan, J.; Lei, T.; Kim, H. R.; Song, Y. I.; *et al.* Roll-to-Roll Production of 30-in. Graphene Films for Transparent Electrodes. *Nat. Nanotechnol.* **2010,** *5*, 574–578.
33. Egerton, P. L.; Hyde, E. M.; Trigg, J.; Payne, A.; Mijovic, M. V.; Reiser, A. Photocycloaddition in Liquid Ethyl Cinnamate and in Ethyl Cinnamate Glasses. The Photoreaction as a Probe into the Micromorphology of the Solid. *J. Am. Chem. Soc.* **1981,** *103*, 3859–3863.
34. Huh, S.; Kim, S. B. Fabrication of Conducting Polymer Films Containing Gold Nanoparticles with Photo-Induced Patterning. *J. Phys. Chem. C* **2010,** *114*, 2880–2885.
35. Pisana, S.; Lazzeri, M.; Casiraghi, C.; Novoselov, K. S.; Geim, A. K.; Ferrari, A. C.; Mauri, F. Breakdown of the Adiabatic Born–Oppenheimer Approximation in Graphene. *Nat. Mater.* **2007,** *6*, 198–201.
36. Das, A.; Pisana, S.; Chakraborty, B.; Piscanec, S.; Saha, S. K.; Waghmare, U. V.; Novoselov, K. S.; Krishnamurthy, H. R.; Geim, A. K.; Ferrari, A. C.; *et al.* Monitoring Dopants by Raman Scattering in an Electrochemically Top-Gated Graphene Transistor. *Nat. Nanotechnol.* **2008,** *3*, 210–215.
37. Huh, S.; Chae, B.; Kim, S. B. Two Strategies for the Self-Assembly of Gold Nanoparticles: Photoreaction and Radical Reaction. *J. Colloid Interface Sci.* **2008,** *327*, 211–215.
38. Porter, L. A., Jr.; Ji, D.; Westcott, S. L.; Graupe, M.; Czernuszewicz, R. S.; Halas, N. J.; Lee, T. R. Gold and Silver Nanoparticles Functionalized by the Adsorption of Dialkyl Disulfides. *Langmuir* **1998,** *14*, 7378–7386.
39. Moskovits, M. Surface-enhanced Raman Spectroscpy. *Rev. Mod. Phys.* **1985,** *57*, 783–826.
40. Kneipp, K.; Kneipp, H.; Itzkan, I.; Dasari, R. R.; Feld, M. S. Ultrasensitive Chemical Analysis by Raman Spectroscopy. *Chem. Rev.* **1999,** *99*, 2957–2975.
41. Kim, N.; Oh, M. K.; Park, S.; Kim, S. K.; Hong, B. H. Effect of Gold Substrates on the Raman Spectra of Graphene. *Bull. Korean Chem. Soc.* **2010,** *31*, 999–1003.
42. Schedin, F.; Lidorikis, E.; Lombardo, A.; Kravets, V. G.; Geim, A. K.; Grigorenko, A. N.; Novoselov, K. S.; Ferrari, A. C. Surface-Enhanced Raman Spectroscopy of Graphene. *ACS Nano* **2010,** *4*, 5617–5626.
43. Ferrari, A. C.; Meyer, J. C.; Scardaci, V.; Casiraghi, C.; Lazzeri, M.; Mauri, F.; Piscanec, F.; Jiang, D.; Novoselov, K. S.; Roth, S.; *et al.* Raman Spectrum of Graphene and Graphene Layers. *Phys. Rev. Lett.* **2006,** *97*, 187401.
44. Morant, C.; Andrey, J.; Prieto, P.; Mendiola, D.; Sanz, J. M.; Elizalde., E. XPS Characterization of Nitrogen-Doped Carbon Nanotubes. *Phys. Status Solidi A* **2006,** *203*, 1069–1075.
45. McCreary, K. M.; Pi1, K.; Swartz, A. G.; Han, W.; Bao, W.; Lau, C. N.; Guinea, F.; Katsnelson, M. I.; Kawakami, R. K. Effect of Cluster Formation on Graphene Mobility. *Phys. Rev. B* **2010,** *81*, 115453.
46. Pi, K.; Han, W.; McCreary, K. M.; Swartz, A. G.; Li, Y.; Kawakami, R. K. Manipulation of Spin Transport in Graphene by Surface Chemical Doping. *Phys. Rev. Lett.* **2010,** *104*, 187201.
47. Yan, J.; Zhang, Y.; Kim, P.; Pinczuk, A. Electric Field Effect Tuning of Electron-Phonon Coupling in Graphene. *Phys. Rev. Lett.* **2007,** *98*, 166802.
48. Farmer, D. B.; Golizadeh-Mojarad, R.; Perebeinos, V.; Lin, Y. M.; Tulevski, G. S.; Tsang, J. C.; Avouris, P. Chemical Doping and Electron-Hole Conduction Asymmetry in Graphene Devices. *Nano Lett.* **2009,** *9*, 388–392.
49. Brust, M.; Walker, M.; Bethell, D.; Schiffrin, D. J.; Whyman, R. Synthesis of Thiol-derivatised Gold Nanoparticles in a Two-phase Liquid-Liquid System. *J. Chem. Soc., Chem. Commun.* **1994,** *7*, 801–802.
50. Brust, M.; Fink, J.; Bethell, D.; Schiffrin, D. J.; Kiely, C. Synthesis and Reactions of Functionalised Gold Nanoparticles. *J. Chem. Soc., Chem. Commun.* **1995,** *16*, 1655–1656.
51. Lee, W. H.; Cho, J. H.; Cho, K. Control of Mesoscale and Nanoscale Ordering of Organic Semiconductors at the Gate Dielectric/Semiconductor Interface for Organic Transistors. *J. Mater. Chem.* **2010,** *20*, 2549–2561.